Acta Crystallographica Section D
Biological Crystallography
ISSN 0907-4449

Structure of plastocyanin from the cyanobacterium *Anabaena variabilis*

Lars Schmidt, Hans E. M. Christensen and Pernille Harris*

Department of Chemistry, The Technical University of Denmark, Building 207, DK-2800 Kgs. Lyngby, Denmark

Correspondence e-mail: ph@kemi.dtu.dk

Received 30 March 2006
Accepted 20 June 2006

PDB Reference: plastocyanin, 2gim, r2gimsf.

Plastocyanin from the cyanobacterium *Anabaena variabilis* was heterologously produced in *Escherichia coli* and purified. Plate-like crystals were obtained by crystallization in 1.15 *M* trisodium citrate and 7.67 m*M* sodium borate buffer pH 8.5. The crystals belong to the orthorhombic space group $P2_12_12_1$, with unit-cell parameters $a = 67.85$, $b = 45.81$, $c = 63.41$ Å. The structure of the oxidized protein was solved to a resolution of 1.6 Å using plastocyanin from *Phormidium laminosum* as a search model. Two molecules were found in the asymmetric unit. The electrostatic surface of the basic protein showed a large population of positively charged residues in the northern site, whereas the eastern site lacked the two strongly negatively charged patches. The copper ion was found to be relatively mobile and there were two distinct conformations of His61.

1. Introduction

Plastocyanins are small type I blue copper proteins ranging in size from 97 to 105 amino acids (Malkin & Malmström, 1970). They play an essential role in oxygenic photosynthesis, where they act as mobile electron carriers, receiving an electron from cytochrome *f* (Cyt *f*), a subunit of the membrane-bound cytochrome b_6f complex, and donating the electron to the $P700^+$ photoreaction centre of photosystem I (PS I; Davis *et al.*, 1980; Hope, 2000; Redinbo *et al.*, 1994). In fact, about 30% of the total oxygen in the atmosphere is produced by cyanobacteria (Fromme *et al.*, 2001).

Extensive studies of the electron-transfer mechanism of eukaryotic plastocyanins have revealed two surface regions of plastocyanin that are crucial for binding and electron transfer to PS I (Ubbink *et al.*, 1998; Ejdebäck *et al.*, 2000). One region is a strongly negatively charged site (approximately 10–15 Å from the copper centre) on the eastern (or remote) site of the molecule, divided into one large and one small acidic patch. In the sequence alignment in Fig. 1(*a*), sequences from plant plastocyanins in the PDB have been aligned (plastocyanin from the fern *Dryopteris crassirhizoma* has been omitted as it seems to be very different from other higher plants; Kohzuma *et al.*, 1999). These negatively charged regions are seen around residue 43 as highly conserved DED residues and around residue 60 dominated by EED residues. The second region is a hydrophobic surface close to the copper ion (approximately 6 Å) on the northern (or adjacent) site (Badsberg *et al.*, 1996; Illerhaus *et al.*, 2000). This region is seen in Fig. 1(*a*) as the highly conserved C-terminus and as conserved regions close to the N-terminus and around residues 34 and residue 65 (poplar plastocyanin residue numbers). Results from studies in which

© 2006 International Union of Crystallography
Printed in Denmark – all rights reserved

nuclear magnetic resonance (NMR) spectroscopy was used to map the contact surface between Cyt *f* and plastocyanin from spinach support the idea that both the hydrophobic and the acidic patches of plant plastocyanins make contact with Cyt *f* during electron transfer. This indicates that both electrostatic and hydrophobic interactions are important in stabilization of the formed electron-transfer complex (Ejdebäck *et al.*, 2000).

Whereas plastocyanins in higher plants have an overall negative charge (-9 ± 1), prokaryotic plastocyanins are close to neutral and can even be positively charged (Davis *et al.*, 1980; Sykes, 1991). These differing electrostatic properties are a result of the organism-dependent character of the eastern site in plastocyanins. A sequence alignment of the prokaryotic plastocyanins present in the PDB is shown in Fig. 1(*b*). These are seen to lack most of the negatively charged residues at their remote eastern binding sites; some may even be replaced by positively charged residues, resulting in more basic isoelectric points compared with the acidic plastocyanins in higher plants (Davis *et al.*, 1980). The regions responsible for the hydrophobic northern part of the molecule are still conserved, although not to the same extent as in the plant plastocyanins. The two regions at the northern and eastern sites apparently continue to be important for the activity of prokaryotic plastocyanins. Schlarb-Ridley *et al.* (2002) investigated the role of charged residues on the surface of *Phormidium laminosum* plastocyanin from the reaction with Cyt *f in vitro*. They found that whereas Cyt *f* in higher plants and green algae possesses a prominent basic ridge which interacts with the acidic patches in plastocyanins, there is a less prominent acidic ridge present in Cyt *f* from *Ph. laminosum* to interact with the neutral to basic area on *Ph. laminosum* plastocyanin. The crystal structure of a mutant plastocyanin from the cyanobacterium *Synechocystis* sp. PCC6803 was published by Romero *et al.* (1998), who suggested that the absence of an acidic patch could be explained if the electron transfer to the *Synechocystis* plastocyanin occurs *via* a collisional reaction mechanism where no kinetically stable transient complex is detectable.

The 105-amino-acid (10.9 kDa) plastocyanin from the cyanobacterium (blue–green algae) *Anabaena variabilis* has a positive overall charge of +1 at neutral pH (Aitken, 1975) and an isoelectric point of 8.4 (Davis *et al.*, 1980), making it unique and of special interest in structural studies. Solution structures of *A. variabilis* plastocyanin have previously been determined of the reduced form (Badsberg *et al.*, 1996) and the Cu site has been characterized very recently using paramagnetic NMR relaxation restraints (Hansen & Led, 2006). Only two basic plastocyanins are found in the PDB. Both are NMR structures, one being the *A. variabilis* plastocyanin (PDB code 1fa4; Badsberg *et al.*, 1996) and the other being plastocyanin from the cyanobacterium *Prochlorothrix hollandica* (PDB code 2b3i; Babu *et al.*, 1999). The latter has an isoelectric point of 8.1 (Bullerjahn, 2000).

Ma *et al.* (2003) found that the entire copper site and the eastern face in *A. variabilis* plastocyanin are affected by microsecond–millisecond dynamics, corresponding to the time scale of biological electron-transfer reactions involved in the interaction with the reactions partners Cyt *f* and PS I. A characterization of the microsecond–millisecond dynamics of *A. variabilis* plastocyanin using a combined analysis of ^{15}N NMR relaxation and chemical shift (Hass *et al.*, 2004) suggests that the observed microsecond–millisecond dynamics of *A. variabilis* plastocyanin is closely related to the protonation of His61 and His92. His92 is one of the copper ion-binding residues. His61 is not part of the redox centre, but protonation of similar remote histidines is known to influence the redox activity

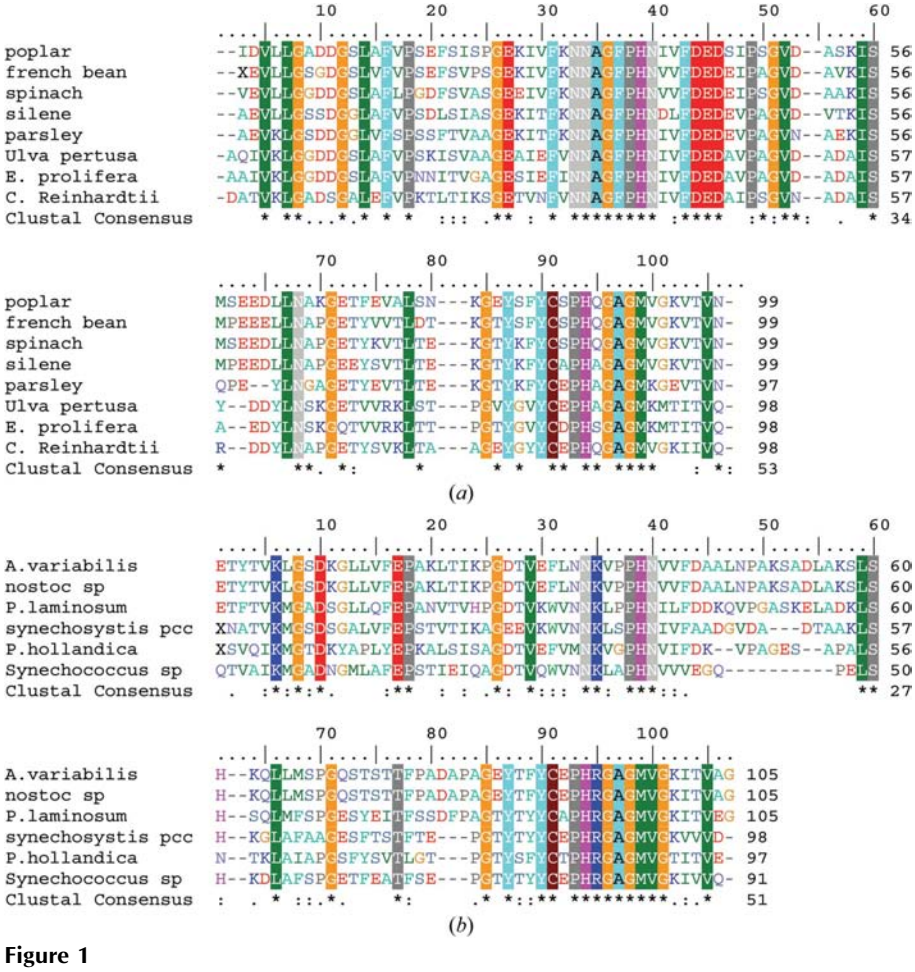

Figure 1
Sequence alignment performed with *ClustalW* (Thompson *et al.*, 1994) and *BioEdit* (Hall, 1999) of plastocyanins found in the PDB. (*a*) Plastocyanins from plants. (*b*) Plastocyanins from cyanobacteria. Colour scheme: MVLI, green; G, orange; ED, red; RK, blue; STQN, light blue; AFY, turquoize; H, lilac; P, grey; C, brown.

Table 1
Data-collection statistics.

Values in parentheses refer to the highest resolution shell.

Beamline	I711, MAX II, Sweden
Detector	MAR Research CCD
Wavelength (Å)	1.11
Temperature (K)	100
Space group	$P2_12_12_1$
Unit-cell parameters† (Å)	a = 67.85, b = 45.81, c = 63.41
Resolution range (Å)	20–1.55 (1.8–1.55)
No. of reflections	175468 (55390)
No. of unique reflections	24943 (7815)
Mosaicity (°)	0.4–0.5
Redundancy	7.03 (7.09)
Completeness (%)	93.3 (99.8)
$I/\sigma(I)$	12.71 (5.02)
$R_{\rm int}$ (%)	10.7 (39.8)
Solvent content (%)	43.8

† Note that a non-standard setting has been used for the unit-cell parameters.

in several blue copper proteins (Canters *et al.*, 2000; Dennison & Lawler, 2001; Kalverda *et al.*, 1999; Sato & Dennison, 2002; Sigfridsson *et al.*, 1995). Hence, the protonation of these histidines may provide plastocyanins and other blue copper proteins with an important regulatory mechanism (Hass *et al.*, 2004).

2. Experimental

2.1. Overexpression and purification of *A. variabilis* plastocyanin

A. variabilis plastocyanin was heterologously produced in *Escherichia coli* from the previously described strain (Hass *et al.*, 2004) by fed-batch cultivation as described below.

Pre-cultures were grown overnight from 193 K glycerol stocks on Luria–Bertini (LB) medium agar plates supplemented with 100 mg l^{-1} ampicillin at 310 K. A single colony was used to inoculate 50 ml liquid LB medium supplemented with 100 mg l^{-1} ampicillin and grown at 250 g and 310 K to an OD_{600} of 0.6–1.0 and then kept overnight at 277 K. The cells were sedimented by centrifugation (277 K, 3000*g*, 10 min) and resuspended in fresh LB medium supplemented with 100 mg l^{-1} ampicillin. 6.5 ml of the suspension was then used to inoculate 650 ml LB medium supplemented with 50 mg l^{-1} carbenicillin. This culture was incubated at 310 K and 250*g* to an OD_{600} of 1.5 and the cells were sedimented by centrifugation (277 K, 3000 g, 10 min) and most of the medium decanted off. The remaining 15 ml of medium was used to resuspend the cells and the cell suspension was then used to inoculate the fermentor.

A Biostat B fermentor with a 5 l autoclavable jacketed glass vessel (B. Braun Biotech International) equipped with a Mettler Toledo dissolved dioxygen sensor and a Mettler Toledo gel combination pH electrode was used. Prior to autoclaving, the pH electrode was calibrated. Fermentation data were collected using the *FoxyLogic Fermentation Control Program* v.4.3. During cultivation, the temperature was maintained at 303 K and the pH at 6.8 ± 0.1 by PID-controlled addition of 1 *M* sodium hydroxide. Adjustment of the zero point and the 100% setting of the dioxygen electrode were performed after flushing the fermentor with dinitrogen and with a 5 l min^{-1} flow rate of air at a stirrer speed of 800 rev min^{-1}, respectively. The level of dissolved dioxygen was maintained at 71% by using a double cascade in which the stirrer speed was first increased to a maximum of 800 rev min^{-1} followed by a gas-mix mode where the airflow was enriched with pure dioxygen to maintain the required level of dissolved dioxygen in the medium. The gas flow was maintained at 5 l min^{-1}. Fourfold diluted Antifoam B (Sigma–Aldrich, A5757) was added to a concentration of 20 ppm at the onset of fermentation and then automatically added as required throughout the fermentation.

The synthetic 2.0 l initial batch medium contained (i) 39.0 g KH_2PO_4, 39.3 g $K_2HPO_4{\cdot}3H_2O$, 38.8 g $Na_2HPO_4{\cdot}2H_2O$, 5.87 g Na_2SO_4, 3.00 g NH_4Cl, (ii) 6.1 g $MgCl_2{\cdot}6H_2O$, (iii) 30 ml trace-element stock solution, (iv) 30 ml vitamin solution, (v) 18 ml 5 mg ml^{-1} thiamine–HCl and (vi) 100 mg l^{-1} ampicillin. Components (i) and (ii) were autoclaved separately, while components (iii)–(vi) were added as filter-sterilized solutions. The recipe for the medium is based on the work of Cai *et al.* (1998). The trace-element stock solution contained 0.50 g Na_2EDTA, 0.60 g $CaCl_2{\cdot}2H_2O$, 0.08 g $CoCl_2{\cdot}6H_2O$, 0.12 g $MnCl_2{\cdot}2H_2O$, 0.03 g $CuCl_2{\cdot}2H_2O$, 0.002 g H_3BO_3, 0.070 g $ZnSO_4{\cdot}7H_2O$ and 0.60 g $FeSO_4{\cdot}7H_2O$ per 100 ml. The salts were added to 70 ml water in the order given and the pH was adjusted to 5 with 5 *M* NaOH and to 6.5 with 1 *M* NaOH; finally, the volume was adjusted to 100 ml. The vitamin stock solution contained 10 mg biotin, 10 mg choline chloride, 10 mg folic acid, 10 mg niacinamide, 10 mg calcium D-pantothenate, 10 mg pyridoxal 5-phosphoric acid and 1 mg riboflavin per 100 ml (Venters *et al.*, 1995) and the pH was adjusted to 7 with 1 *M* NaOH.

1 l of feed solution containing 28 g glucose per litre was exponentially fed to the fermentor over 18 h. When the glucose was depleted, 4.5 g NH_4Cl and 8.0 g glucose were added and the culture was induced by addition of IPTG to a final concentration of 0.1 m*M* from a 200 m*M* stock solution. After 2 h, cells were harvested by centrifugation at 3000*g* for 15 min at 277 K, washed with 5 m*M* MES–NaOH pH 6.5 and stored at 193 K until isolation and purification of the protein was initiated.

Recombinant *A. variabilis* plastocyanin was purified as previously described (Hass *et al.*, 2004), with the exception that 1.5 m*M* $CuSO_4$ was added and the solution was incubated overnight.

Approximately 90 mg per litre of culture of pure plastocyanin with a peak ratio of A_{278}/A_{597} of 1.18 was obtained and the protein was stored at 277 K in 5 m*M* MES–NaOH pH 6.5 at a concentration of 9.1 mg ml^{-1} for crystallization experiments. The oxidized form of the recombinant *A. variabilis* plastocyanin is produced with an N-terminal methionine.

2.2. Crystallization and data collection

Crystals of *A. variabilis* plastocyanin were grown using the sitting-drop vapour-diffusion method. The 1 ml reservoir

Table 2
Refinement statistics.

Values in parentheses refer to the highest resolution shell.

Resolution range	20–1.6 (1.8–1.6)
R	0.209
R_{free}	0.260
No. of protein atoms	
Peptide chains	1600
Cu ions	2
No. of solvent molecules	315
No. of reflections in working set	23695
No. of reflections in test set	1249
Mean temperature (B) factors (Å^2)	
Peptide chains	16.6
Cu ions	18.1
Solvent	26.9
R.m.s.d. bond lengths (Å)	0.02
R.m.s.d. bond angles (°)	1.9
R.m.s.d. dihedral angles (°)	0.9
Ramachandran plot	
Most favoured region (%)	91.4
Additionally allowed regions (%)	8.6
Generously allowed regions (%)	0.0
Disallowed regions (%)	0.0

Table 3
Secondary structure of *A. variabilis* plastocyanin.

Secondary-structure element	Crystal structure at 1.6 Å resolution	NMR solution structures†
β-Sheet I		
β-Strand 1	Thr2–Leu7	Thr2–Leu7
β-Strand 2	Phe16–Glu17	Leu14–Pro18
β-Strand 4	Asp27–Asn33	Asp27–Asn33
β-Strand 6	Ser71–Phe76	Gln70–Phe76
β-Sheet II		
β-Strand 3	Lys20–Ile23	Lys20–Lys24
β-Strand 5	Val41–Phe43	Pro37–Asp44
β-Strand 7	Gly83–Tyr88	Gly83–Cys89
β-Strand 8	Val98–Val104	Met97–Ala104
Other β-strands		
β-Strand 9	—	Gln63–Ser67
Helical regions		
α-Helix 1	Ala53–Leu59	Ala53–Ser60

† From Badsberg *et al.* (1996).

contained 1.15 *M* trisodium citrate, 7.67 m*M* sodium borate buffer pH 8.5 (adjusted with 5 *M* HCl) and was optimized from Stura Footprint Screen 1 condition No. 6 (Molecular Dimensions Ltd). The drop was set up with 2 µl protein solution (9.1 mg ml^{-1}, ε_{597} = 4500 M^{-1} cm^{-1}) and 2 µl reservoir solution. Blue plate-shaped crystals grew in clusters from a single nucleation point within 5–7 d at 295 K.

Several large plate-shaped crystals were transferred to a cryoprotectant solution containing 1.5 *M* trisodium citrate, 10 m*M* sodium borate buffer pH 8.5 and separated to approximate dimensions of 0.1 × 0.1 × 0.02 mm. The crystals were mounted in appropriate cryoloops and cooled in liquid nitrogen. Diffraction data were recorded at beamline I711 at MAX-lab, Lund University, Sweden (Table 1).

The crystals appeared to have a relatively large mosaicity and diffracted to about 2 Å. By blocking the nitrogen stream once for a short period of time, the crystals were annealed (Harp *et al.*, 1999), increasing the diffraction limits and simultaneously decreasing the mosaicity. However, multiple rounds of warming and re-flash-cooling (similar to flash-annealing; Yeh & Hol, 1998) did damage the crystals. Data were measured to a resolution of 1.55 Å.

Integration, scaling and merging of the intensities were carried out using *XDS* and *XSCALE* (Kabsch, 1993). Data points around ice rings were removed. Data-collection statistics are presented in Table 1.

2.3. Structure determination and refinement

The crystal structure of *A. variabilis* plastocyanin in its oxidized form was solved by molecular replacement using *MOLREP* (Vagin & Teplyakov, 1997) from the *CCP*4 program suite (Collaborative Computational Project, Number 4, 1994). The amino-acid sequence of *A. variabilis* plastocyanin is 63% identical to that of *Ph. laminosum* plastocyanin, with no insertions, terminal extensions or deletions, and the search model was taken from the crystal structure of *Ph. laminosum* plastocyanin at 2.8 Å resolution (PDB code 1baw; Bond *et al.*, 1999).

A solution with two molecules in the asymmetric unit was obtained in space group $P2_12_12_1$ (correlation factor = 0.54, R = 0.53).

The program *REFMAC*5 (Murshudov *et al.*, 1997) from the *CCP*4 suite was used for refinement cycles and simulated annealing was carried out using *CNS* (Brünger *et al.*, 1998). Rebuilding was performed using the program *WinCoot* (Emsley & Cowtan, 2004). All refinement steps were monitored using an R_{free} value based on 5% of independent reflections.

Difference electron density appeared at the N-terminus and each N-terminus had to be extended with a methionine during refinement.

A total of 315 water molecules were included in the model. Several larger solvent electron densities were identified and attempts to distinguish between solvent molecules and ions from the sodium citrate buffer or the MES–NaOH buffer were made. However, these were unsuccessful.

The observed electron density provided indications of more than one conformation of several residues. Two distinct conformations were modelled for His61 in both chains; however, modelling the apparent alternate conformations of Pro37 and Pro38 did not further improve the R_{free} factor. Finally, the electron densities of the two Met0 extensions indicate a high flexibility. Refinement statistics are presented in Table 2.

The quality of the model was tested using the *BIOTECH* validation suite (Pontius *et al.*, 1996; Vriend, 1990) and *PROCHECK* (Laskowski *et al.*, 1993).

3. Results and discussion

3.1. Overall structure of *A. variabilis* plastocyanin

The final model describes two monomers (chains *A* and *C*) in the asymmetric unit, each containing 106 residues (including Met0). To date, all plastocyanin structures deter-

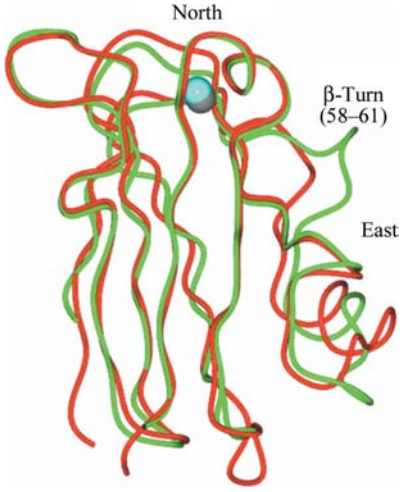

Figure 2
Superimposed structures of *A. variabilis* plastocyanin (red and cyan) and poplar plastocyanin (green and grey; PDB code 1plc; Guss *et al.*, 1992). The structures are represented by the C^{α} atoms and the Cu ions. 58–61 refer to the residues Ser58–Asp61 in poplar plastocyanin. The figure was prepared using *CCP*4*mg* (Potterton *et al.*, 2002).

mined by X-ray diffraction in the PDB have been acidic proteins with an overall negative charge at neutral pH, making plastocyanin from *A. variabilis* the first of its kind. The overall fold of *A. variabilis* plastocyanin follows that of other structurally characterized plastocyanins (Fig. 1). It is dominated by two β-sheets, each containing four β-strands (Table 3). The two β-sheets fold into an antiparallel β-barrel with a hydrophobic core and the loops and turns connecting the β-strands form the two ends of the barrel. We find a secondary structure that deviates slightly from the previously determined solution structures (Badsberg *et al.*, 1996), as presented in Table 3. Most striking is a β-strand which in the NMR structure is found in the eastern region just after the α-helix, as observed in parsley and poplar plastocyanins (Bagby *et al.*, 1994; Guss *et al.*, 1992). This β-strand cannot be assigned in the crystal structure, but comparison is difficult in this area partly because it is not a well defined part of the NMR structure and partly because in the crystal structure the backbone N of Leu64 is hydrogen bonded to the C-terminal O of Gly105 through crystal contacts.

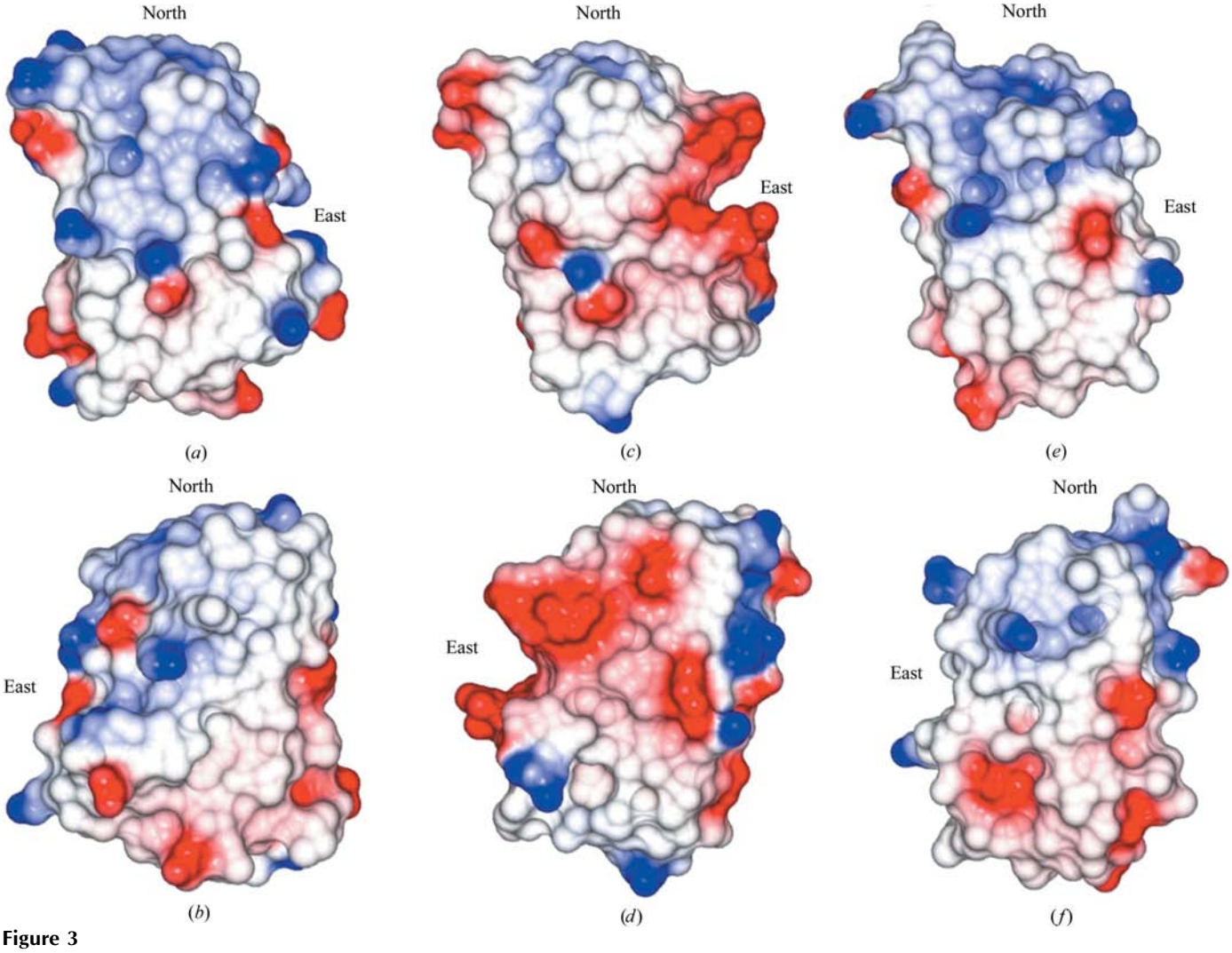

Figure 3
Electrostatic surfaces at different orientations of (*a*) and (*b*) *A. variabilis* plastocyanin, (*c*) and (*d*) poplar plastocyanin (PDB code 1plc; Guss *et al.*, 1992) and (*e*) and (*f*) *Pr. hollandica* plastocyanin (PDB code 2b3i; Babu *et al.*, 1999). Blue, white and red colours represent positive, neutral and negative charge, respectively. The plots were prepared using *CCP*4*mg* (Potterton *et al.*, 2002).

Table 4
Copper binding-site distances (Å) in *A. variabilis* plastocyanin.

Residue numbers in parentheses indicate the corresponding labels in poplar plastocyanin.

	1.6 Å crystal structure (oxidized form)			
	Chain *A*	Chain *C*	Paramagnetic NMR determination (reduced form)†	Poplar plastocyanin 1.33 Å crystal structure‡
Cu—N^{δ} His39(37)	2.07	1.99	1.94 ± 0.01	1.91 ± 0.04
Cu—S^{γ} Cys89(84)	2.13	2.23	2.12 ± 0.03	2.07 ± 0.04
Cu—N^{δ} His92(87)	2.10	2.07	1.98 ± 0.01	2.06 ± 0.04
Cu—S^{δ} Met97(92)	2.77	2.72	2.80 ± 0.04	2.82 ± 0.04

† From Hansen & Led (2006). ‡ From Guss *et al.* (1992).

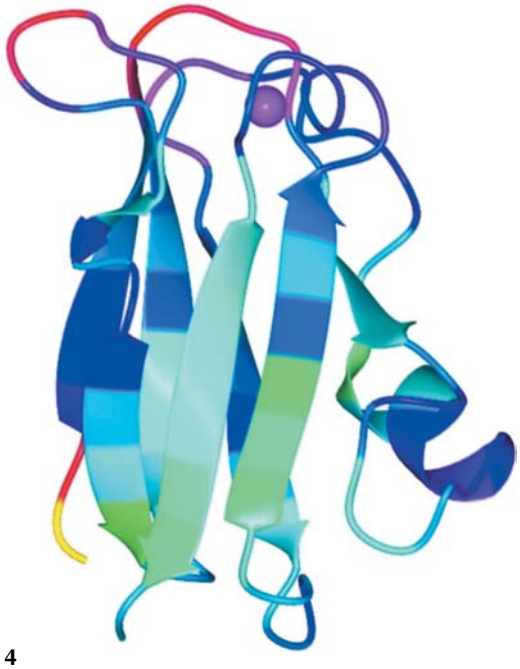

Figure 4
Mapping of the temperature factors of *A. variabilis* plastocyanin. Low, green; mean, blue; high, red; very high, yellow. This figure was prepared using *CCP4mg* (Potterton *et al.*, 2002).

The overall structure is highly conserved between plastocyanins from higher plants and cyanobacteria and the C^{α} traces from all structurally characterized plant plastocyanins (with the exception of *D. crassirhizoma*) may be almost completely aligned. The only significant discrepancy is found for the acidic β-turn, which is only found in the plant plastocyanins that contain the sequence EED (poplar residues 58–60). Structurally, this β-turn is absent in cyanobacteria and in plant plastocyanins without the EED consensus sequence. This results in a displacement of the polypeptide chain in the region (see Fig. 2).

The largest deviations in sequence, structure and electrostatic properties for plant and cyanobacteria plastocyanins are seen in this eastern region, which is highly negatively charged in plastocyanins from higher plants. Plastocyanins from cyanobacteria generally lack the two strongly negatively charged patches. *A. variabilis* plastocyanin, which is positively charged, as may be seen in Fig. 3, furthermore has a large population of positively charged residues at the north end, so that the overall positive charge of the protein primarily is caused by the electrostatic properties of the eastern and northern sites, which are believed to be important for the activity of prokaryotic plastocyanins. The north end of *Pr. hollandica* plastocyanin is also dominated by positively charged residues, as illustrated in Fig. 3, but to a lesser extent than observed in *A. variabilis* plastocyanin.

3.2. Mobility in the northern and eastern site

As in all other plastocyanins, the copper site in *A. variabilis* plastocyanin is located in a hydrophobic pocket at the north end of the molecule (Fig. 2). The copper ion is coordinated as a type I blue copper to four ligands in a distorted tetrahedral

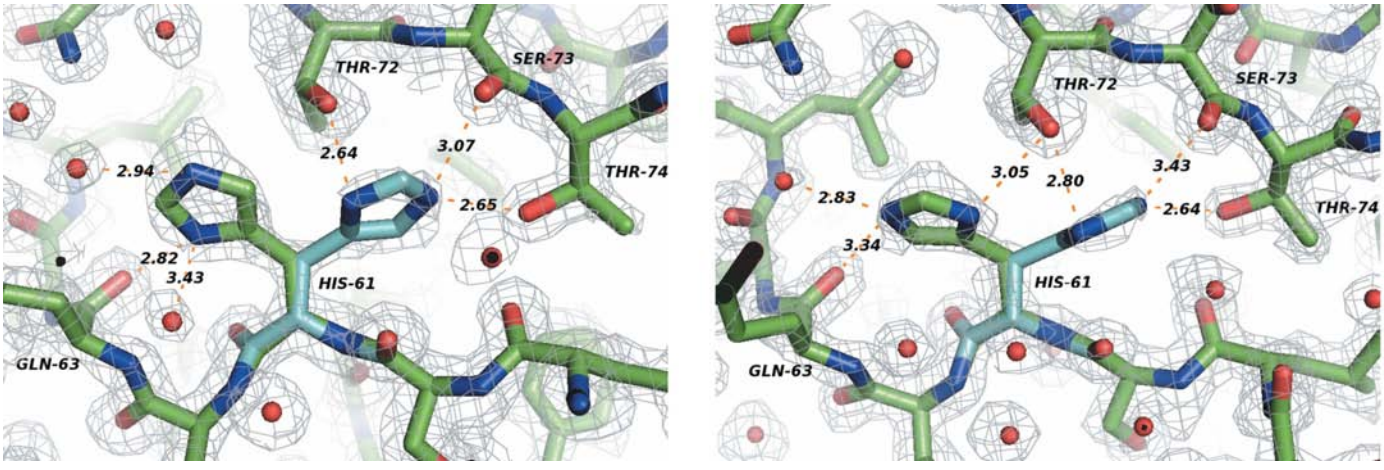

Figure 5
$2F_{obs} - F_{calc}$ σ_A-weighted electron-density map showing the hydrogen-bonding networks of the two conformations of His61 in *A. variabilis* chains *A* (left) and *C* (right). The higher occupied (occupancy 0.55 in chain *A* and 0.65 in chain *C*) conformations are shown in green (C-atom colour) and the lower occupied (0.45 in chain *A* and 0.35 in chain *C*) are shown in light blue. This figure was produced using *PyMOL* (DeLano, 2002).

configuration. The four ligands are His39, Cys89, His92 and one typically weakly bound Met97 with a long bond length (Table 4). These four ligands are conserved in plastocyanins of known sequence (Redinbo *et al.*, 1994). The coordinating distances are comparable to those of poplar plastocyanin, as given in Table 4. For comparison, the distances found recently by paramagnetic NMR are also listed.

In Fig. 4, a mapping is shown of the temperature factors of *A. variabilis* plastocyanin. It is seen that the northern end of the protein molecule surrounding the Cu ion has the highest thermal parameters. This indicates a relatively flexible north region dominated by loops and turns including a mobile copper ion. The loop between β-strands 4 and 5 containing residues Asn34–Pro38 has an average temperature factor of 23.1 Å^2. The enhanced flexibility of this region closely located to the copper ion could be caused by the apparent alternate conformations of Pro37 and Pro38. The crystal structure of *A. variabilis* plastocyanin confirms the previously suggested *cis*-peptide bonds for Pro18 and Pro38 (Badsberg *et al.*, 1996). However, the apparent alternate conformations of Pro37 and Pro38 suggests the presence of both a *cis* and a *trans* conformation of the Pro37–Pro38 bond as proposed previously by Ma *et al.* (2001). The mobilities of Pro37 and Pro38 do not seem to have a significant effect on His39 coordination of the copper ion.

The average temperature factors (or *B* values) of the four copper ion ligands, His39, Cys89, His92 and Met97, are 14.8, 16.1, 15.2 and 13.4 Å^2, respectively, in comparison to 18.1 Å for the Cu ions. A larger thermal parameter for copper than for the four liganding residues has been observed in several other plastocyanins, including that from *Chlamydomonas reinhardtii* (Redinbo *et al.*, 1993). This could imply that the microsecond–millisecond dynamics of the active-site region found previously (Ma *et al.*, 2003) are primarily caused by a mobile copper ion. This copper flexibility might be necessary in order to ensure the most favourable conformation during electron transfer upon complex formation and low reorganization energy when going from the reduced to the oxidized form (Ma *et al.*, 2003). It has been hypothesized that the oxidized copper(II) forms of blue copper proteins are at least partially reduced to the copper(I) state during diffraction experiments owing to radiation damage (Carugo & Carugo, 2005). This might explain to some extent the apparent mobility of the copper site. Three of the ligands, Cys89, His92 and Met97, are all part of the stabilizing loop with a high resemblance to an α-helix located between β-strands 7 and 8.

Previous studies (Hass *et al.*, 2004; Ma *et al.*, 2003) have further indicated enhanced flexibility in the south-eastern corner, which includes the α-helix. The average temperature factor for residues Asp44–Lys51, corresponding to the large acidic patch in eukaryotic plastocyanins, is 17.2 Å^2, while the average temperature factor for residues His61–Gln63, which correspond to the small acidic patch in eukaryotic plastocyanins, is 17.7 Å^2 (with two modelled conformations of His61). These averaged temperature factors should be compared with the overall *B* factor of 16.6 Å^2 and do not indicate a significant enhanced mobility in the eastern regions, which are regarded as important for the activity of prokaryotic plastocyanins such as *A. variabilis* plastocyanin. If, however, we make a structural alignment of the cyanobacteria plastocyanins solved from X-ray structures, these show the largest deviations in this area and it may be that the rigid structure we observe is an artefact from the crystal surroundings. Ma *et al.* (2003) furthermore observed a relatively loose structure of the β-strand Gln63–Ser67, which was also not found in the crystal structure. The residues Lys62, Gln63, Ser67, Pro68 and Gly69 all have average temperature factors between 19.6 and 21.2 Å^2, which is somewhat above the average *B* factor for the peptide and could correspond to a relatively flexible region.

3.3. Double conformation of His61

The residues His61–Gln63 cluster around the imidazole ring of His61, together with Thr72–Thr74, and the two modelled conformations of His61 give rise to different hydrogen-bonding networks, as illustrated in Fig. 5. The conformation with a hydrogen-bonding contact to Gln63 is slightly favoured by the ratios 0.55:0.45 and 0.65:0.35 in the two chains *A* and *C*, respectively. An analysis of the hydrogen-bonding possibilities using *WHATIF* (Vriend, 1990) suggested different orientations in the *A* and *C* chains of the major component of the imidazole group (as illustrated in Fig. 5). This means that we cannot establish from the X-ray data alone whether one orientation of the imidazole ring is more likely than the other or if both are actually present. Furthermore, the side chains of the major conformation of His61 in the *A* and *C* chains do not superimpose very well, also indicating a large flexibility of this residue. The less occupied conformation of His61 seems to have a more well defined orientation, with identical hydrogen-bonding contacts in the two molecules of the asymmetric unit.

The double conformation of His61 may be a confirmation of previous studies using a combined analysis of ^{15}N NMR relaxation and chemical shift of the conformational changes in *A. variabilis* plastocyanin induced by histidine protonation (Hass *et al.*, 2004). Here it was suggested that His61, which is located approximately 9 Å from the copper ion, is not only a part of the small acidic patch at the eastern site of the molecule but also appears to have a direct coupling to the active site that is affected by its protonation. The average pK_a values for His92 and His61 were determined to be 5.09 $\pm$ 0.01 and 7.06 $\pm$ 0.02, respectively, and it was found that residues close to the imidazole group of His61 have large R_2 relaxation rates of the backbone at a pH of around 7. This corresponds to the pH value where interconversion between the protonated and deprotonated forms of His61 is effective. Hass and coworkers suggested that an additional exchange process which only involves the deprotonated form of His61 could affect the orientation of the His61 side chain and tautomerization and/or rearrangement of the hydrogen bonding of the aromatic N—H of the imidazole group. During the nucleation and crystal growth a change in pH from 6.5 (5 m*M* MES–NaOH) towards 8.5 (reservoir solution) may have induced an interconversion of His61. However, it is not a certainty at this point that the double conformation of His61 arises from interconversion of

protonated and deprotronated forms. The crystal structure shows no general displacement of surrounding residues owing to the double conformation of His61. If the different conformations of His61 are to be studied more thoroughly, higher resolution data are likely to be needed at various pH values. No indications of any conformational changes of His92 were observed in the crystal structure of oxidized *A. variabilis* plastocyanin, but future studies of the reduced form might help elucidate the exchange process during protonation and deprotonation of His92.

The authors are grateful to MAX-lab, Lund, Sweden for providing beam time for the project and to DANSYNC and the EU for contribution to travel expenses under the 'Access to Research Infrastructure' program.

References

Aitken, A. (1975). *Biochem. J.* **149**, 675–683.
Babu, C. R., Volkman, B. F. & Bullerjahn, G. S. (1999). *Biochemistry*, **38**, 4988–4995.
Badsberg, U., Jørgensen, A. M. M., Gesmar, H., Led, J. J., Hammerstad, J. M., Jespersen, L.-L. & Ulstrup, J. (1996). *Biochemistry*, **35**, 7021–7031.
Bagby, S., Driscoll, P. C., Harvey, T. S. & Hill, H. A. O. (1994). *Biochemistry*, **33**, 6611–6622.
Bond, C. S., Bendall, D. S., Freeman, H. C., Guss, J. M., Howe, C. J., Wagner, M. J. & Wilce, M. C. J. (1999). *Acta Cryst.* D**55**, 414–421.
Brünger, A. T., Adams, P. D., Clore, G. M., DeLano, W. L., Gros, P., Grosse-Kunstleve, R. W., Jiang, J.-S., Kuszewski, J., Nilges, M., Pannu, N. S., Read, R. J., Rice, L. M., Simonson, T. & Warren, G. L. (1998). *Acta Cryst.* D**54**, 905–921.
Bullerjahn, G. S. (2000). *The Spectrum*, **13**(4), 1–6.
Cai, M., Huang, Y., Sakaguchi, K., Clore, G. M., Gronenborn, A. M. & Craigie, R. (1998). *J. Biomol. NMR*, **11**, 97–102.
Canters, G. W., Kolczak, U., Armstrong, F., Jeuken, L. J. C., Camba, R. & Sola, M. (2000). *Faraday Discuss.* **116**, 205–220.
Carugo, O. & Carugo, K. D. (2005). *Trends Biochem. Sci.* **30**, 213–219.
Collaborative Computational Project, Number 4 (1994). *Acta Cryst.* D**50**, 760–763.
Davis, D. J., Krogmann, D. W. & Pietro, A. S. (1980). *Plant Physiol.* **65**, 697–702.
DeLano, W. L. (2002). *The PyMOL Molecular Visualization System.* DeLano Scientific, San Carlos, CA, USA. http://www.pymol.org.
Dennison, C. & Lawler, A. T. (2001). *Biochemistry*, **40**, 3158–3166.
Ejdebäck, M., Bergkvist, A., Karlsson, B. G. & Ubbink, M. (2000). *Biochemistry*, **39**, 5022–5027.
Emsley, P. & Cowtan, K. (2004). *Acta Cryst.* D**60**, 2126–2132.
Fromme, P., Jordan, P. & Krauss, N. (2001). *Biochim. Biophys. Acta*, **1507**, 5–31.
Guss, J. M., Bartunik, H. D. & Freeman, H. C. (1992). *Acta Cryst.* B**48**, 790–811.
Hall, T. A. (1999). *Nucleic Acids Symp. Ser.* **41**, 95–98.
Hansen, D. F. & Led, J. J. (2006). *Proc. Natl Acad. Sci. USA*, **103**, 1738–1743.
Harp, J. M., Hanson, B. L., Timm, D. E. & Bunick, G. J. (1999). *Acta Cryst.* D**55**, 1329–1334.
Hass, M. A. S., Thuesen, M. H., Christensen, H. E. M. & Led, J. J. (2004). *J. Am. Chem. Soc.* **126**, 753–765.
Hope, A. B. (2000). *Biochim. Biophys. Acta*, **1456**, 5–26.
Illerhaus, J., Altschmied, L., Reichert, J., Zak, E., Herrmann, R. G. & Haehnel, W. (2000). *J. Biol. Chem.* **23**, 17590–17595.
Kabsch, W. (1993). *J. Appl. Cryst.* **26**, 795–800.
Kalverda, A. P., Ubbink, M., Gilardi, G., Wijmenga, S. S., Crawford, A., Jeuken, L. J. C. & Canters, G. W. (1999). *Biochemistry*, **38**, 12690–12697.
Kohzuma, T., Inoue, T., Yoshizaki, F., Sasakawa, Y., Onodera, K., Nagatomo, S., Kitagawa, T., Uzawa, S., Isobe, Y., Sugimura, Y., Gotowda, M. & Kai, Y. (1999). *J. Biol. Chem.* **274**, 11817–11823.
Laskowski, R. A., MacArthur, M. W., Moss, D. S. & Thornton, J. M. (1993). *J. Appl. Cryst.* **26**, 283–291.
Ma, L., Hass, M. A. S., Vierick, N., Kristensen, S. M., Ulstrup, J. & Led, J. J. (2003). *Biochemistry*, **42**, 320–330.
Ma, L., Philipp, E. & Led, J. J. (2001). *J. Biomol. NMR*, **19**, 199–208.
Malkin, R. & Malmström, B. G. (1970). *Adv. Enzymol.* **33**, 177–244.
Murshudov, G. N., Vagin, A. A. & Dodson, E. J. (1997). *Acta Cryst.* D**53**, 240–255.
Pontius, J., Richelle, J. & Wodak, S. J. (1996). *J. Mol. Biol.* **264**, 121–136.
Potterton, E., McNicholas, S., Krissinel, E., Cowtan, K. & Noble, M. (2002). *Acta Cryst.* D**58**, 1955–1957.
Redinbo, M. R., Cascio, D., Choukair, M. K., Rice, D., Merchant, S. & Yeates, T. O. (1993). *Biochemistry*, **32**, 10560–10567.
Redinbo, M. R., Yeates, T. O. & Merchant, S. (1994). *J. Bioenerg. Biomembr.* **26**, 49–66.
Romero, A., de la Cerda, B., Varela, P. F., Navarro, J. A., Hervás, M. & de la Rosa, M. A. (1998). *J. Mol. Biol.* **275**, 327–336.
Sato, K. & Dennison, C. (2002). *Biochemistry*, **41**, 120–130.
Schlarb-Ridley, B. G., Bendall, D. S. & Howe, C. J. (2002). *Biochemistry*, **41**, 3279–3285.
Sigfridsson, K., Hansson, Ö., Karlsson, B. G., Baltzer, L., Nordling, M. & Lundberg, L. G. (1995). *Biochim. Biophys. Acta*, **1228**, 28–36.
Sykes, A. G. (1991). *Adv. Inorg. Chem.* **36**, 377–408.
Thompson, J. D., Higgins, D. G. & Gibson, T. J. (1994). *Nucleic Acids Res.* **22**, 4673–4680.
Ubbink, M., Edjebäck, M., Karlsson, B. G. & Bendall, D. S. (1998). *Structure*, **6**, 323–335.
Vagin, A. & Teplyakov, A. (1997). *J. Appl. Cryst.* **30**, 1022–1025.
Venters, R. A., Huang, C.-C., Farmer, B. T. II, Trolard, R., Spicer, L. D. & Fierke, C. A. (1995). *J. Biomol. NMR*, **5**, 339–344.
Vriend, G. (1990). *J. Mol. Graph.* **8**, 52–56.
Yeh, J. I. & Hol, W. G. J. (1998). *Acta Cryst.* D**54**, 479–480.